

Reversible NMO

William A. Burnett* and Robert J. Ferguson

ABSTRACT

The nonstationary equivalent of the Fourier shift results in a general one-dimensional integral transform that applies to many seismic data processing steps. This general transform is, computationally, a simple matrix-vector multiplication, and it is a tool for implementation. Here, this general transform is used to implement a reversible normal moveout (NMO) correction.

INTRODUCTION

The normal moveout (NMO) correction is one of the fundamental operations of seismic data processing, (Dobrin and Savit, 1988). It can be formulated from wave theory in ways to account for anisotropy and heterogeneity, or it can be approximated from geometric arguments and middle school mathematics. We will gladly take the latter approach here, and then implement the familiar second order NMO equation using the data processing transform. Just as the Fourier transform was used to demonstrate the principles used in the theory and implementation of the data processing transform, NMO will serve as a familiar example and as a guide for implementing other processing steps by integral transform.

The conventional approach to implementing NMO requires interpolation between samples in time, and this is demonstrably a fast but irreversible tool, (Burnett, 2007). It is helpful here to review basic NMO theory before proceeding to the NMO integral transform.

THEORY

One of the preliminary goals of seismic data processing is to prepare the acquired data for migration. Many migration algorithms, particularly post-stack, assume that the input data are acquired at zero-offset. This is of course physically impractical, but data acquired at various offsets can be processed into data that one would expect to record at zero-offset. The two major steps that accomplish this are the NMO correction, and the dip-moveout (DMO) correction, (Dobrin and Savit, 1988). NMO also serves a purpose in all processing flows, even pre-stack migration processing flows, as the primary tool for estimating the subsurface velocity model.

Assuming homogeneity and isotropy, the reasoning behind the NMO correction and the derivation of the second order NMO equation can be seen with a simple picture of a seismic experiment. As seen in Figure 1, energy travels away from the source in every direction. The first arrival of the energy at nearby receivers travels straight toward them along the Earth's surface. The different receivers record this direct arrival energy at times that are linearly proportional to their respective offsets from the source. When raw seismic data is displayed as recording time versus offset, a linear pattern manifests due to the direct-arrival

*University of Texas, Austin

energy. The direct-arrival is then said to have linear moveout. Energy leaving the source with some downward component may reflect off of interfaces in the subsurface. Now the source to receiver travel path, and therefore the travel time is no longer linearly dependent on offset. For the case of horizontal reflectors, a reasonably normal geologic case, travel time for reflected energy increases hyperbolically with offset. Again displaying the seismic data as travel time versus offset, energy reflected off of interfaces normal (perpendicular) to the depth axis will manifest as hyperbolic patterns. Simple reflections are then said to have hyperbolic, or normal, moveout.

It helps to view a reflection event at each receiver as having an arrival time that is the sum of the equivalent zero-offset time for that receiver, and an offset and time-dependent delay caused by normal moveout:

$$t_x = t_0 + \Delta_{\text{NMO}}. \quad (1)$$

Since the goal is to move the acquired data to its zero-offset equivalent, each event is shifted back in time by its appropriate Δ_{NMO} . This can be found through geometric observations of the seismic experiment. First, take the travel distance of the energy between the source and each receiver as shown in figure 1. The Pythagorean Theorem gives the distance, d , in terms of the reflector depth, z , and the offset, x :

$$d = 2\sqrt{z^2 + \frac{x^2}{4}}. \quad (2)$$

Second, dividing this distance by the velocity, v , at which the energy travelled through the medium gives the total travel time predicted by the simple model. Third, recognizing $2z/v$ the zero-offset travel time, t_0 , arrive at the second order NMO equation for a single reflector:

$$t_x = \sqrt{t_0^2 + \frac{x^2}{v^2}}. \quad (3)$$

This equation is only valid for a single layer model, because then there is only a single velocity, v , specified. For multiple flat-layer models, when the velocity becomes a function of depth, a better velocity to substitute into the NMO equation is the root-mean-square (RMS) velocity. The RMS velocity is a time-weighted average velocity for a layered model, (Dobrin and Savit, 1988). To predict travel *times*, a standard average or even a depth-weighted velocity would be insufficient, because neither account for the actual travel time spent in each individual layer. The RMS velocity for an N-layer model is given as:

$$v_{\text{rms}} = \frac{\sum_{j=1}^N v_j^2 t_j}{\sum_{j=1}^N t_j}. \quad (4)$$

where v_j and t_j are the velocity and travel time, respectively, of the j -th layer. When performing the NMO correction for a layered velocity model, it is important to realize that v_{rms} is a function of time, defined at zero offset. The NMO equation for multiple layers then has the form,

$$t_x = \sqrt{t_0^2 + \frac{x^2}{v_{\text{rms}}^2(t_0)}}. \quad (5)$$

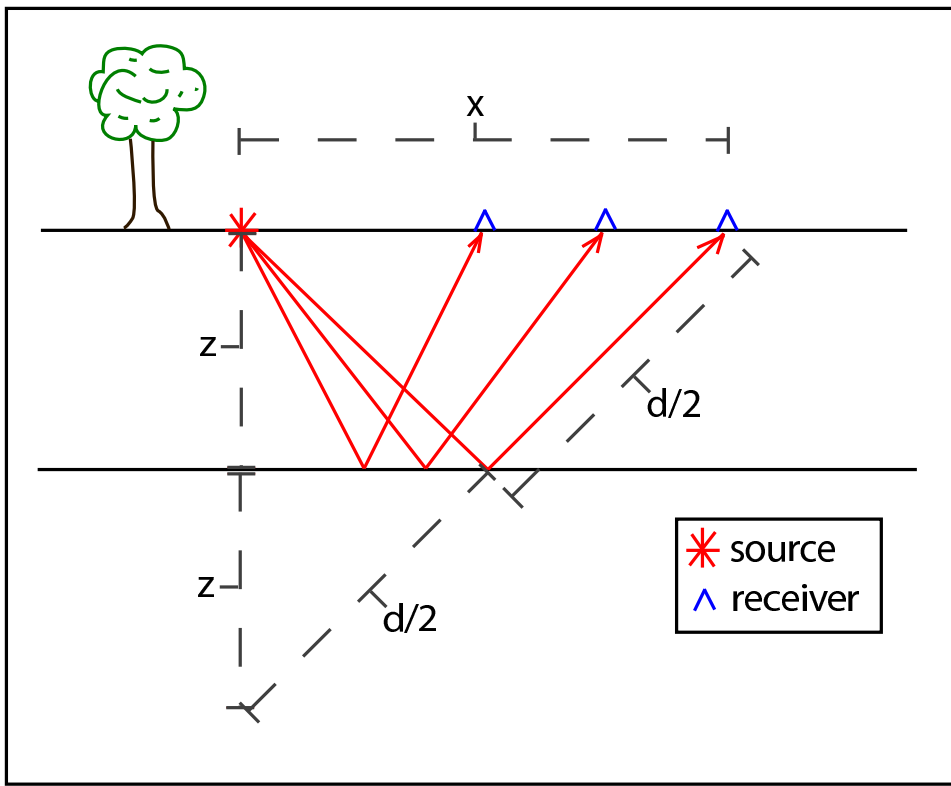


FIG. 1. The seismic experiment. The second order NMO equation is derived from the raypath geometry of this simple single horizontal layer model.

With the introduction of the RMS velocity, the second order NMO equation becomes a useful approximation to the reflection travel times for many simple, but realistic geologic models. For cleaner notation, the RMS velocity used in subsequent expressions is from here on denoted as simply v . We have shown here the simple derivation for an expression to correct data from a single shot, or a shot gather. However, the NMO equation holds for, and is more often applied to, common midpoint (CMP) gathers. Azimuthal and far-offset deviations from hyperbolic moveout behaviour can be caused by anisotropy, but are not predicted by the second order NMO equation. Higher order expressions for the NMO correction can be formulated that account for anisotropy, ((Tsvankin and Thomsen, 1994), (Alkhalifah, 1997)) but we will keep to the admittedly basic case of second order NMO in order to focus on the integral transform development. Nonetheless, even the higher order NMO expressions agree with the form of equation 1, and they could also be implemented by integral transform.

In order to implement the NMO correction by integral transform, we first recognize that NMO is a nonstationary shift. As discussed earlier, the goal is to move the seismic data from its recorded time, t_x to its effective zero offset time, t_0 . Equation 6 gives the nonstationary value of Δ for NMO by integral transform.

$$\Delta_{NMO}(t_0) = t_x(t_0) - t_0. \quad (6)$$

All that is left is to substitute t_x , t_0 , and Δ_{NMO} into the general data processing transform

equation, (Burnett, 2008)

$$h(q) = \frac{1}{2\pi} \int_{-\infty}^{\infty} F(\beta) e^{i\beta p(q)} d\beta, \quad (7)$$

and then calculate α_{NMO} for the inverse transform. The operator matrices can then be constructed for each trace depending on the velocity model and the offset of the trace.

Replacing q with t_0 and p with t_x in, (Burnett, 2008)

$$h(q) \equiv f(q + \Delta(q)) = \frac{1}{2\pi} \int_{-\infty}^{\infty} F(\beta) e^{i\beta\Delta(q)} e^{i\beta q} d\beta, \quad (8)$$

shows the nonstationary shift being applied:

$$h(t_0) \equiv f(t_x) = \frac{1}{2\pi} \int_{-\infty}^{\infty} F(\omega) e^{i\omega\Delta_{NMO}(t_0)} e^{i\omega t_0} d\omega, \quad (9)$$

where ω is now assigned as the Fourier dual of t_0 . In this form of the data processing transform, the shifting and Fourier exponentials are separated. This form provides insight into the shift itself during implementation. Still, combining equations 9 and 6 gives the concise forward NMO transform:

$$h(t_0) \equiv f(t_x) = \frac{1}{2\pi} \int_{-\infty}^{\infty} F(\omega) e^{i\omega t_x} d\omega. \quad (10)$$

This transform maps the uncorrected frequency spectrum of a trace to its appropriate NMO-corrected time series. A key observation at this point is that the output trace is distorted in time with respect to the input, but integration is over frequency, so the forward transform does not account for this distortion.

In the case of the NMO correction, the time distortion is referred to as *NMO stretch* ((Buchholtz, 1972), (Dunkin and Levin, 1973)). This problem manifests is most pronounced at far offsets and early times, where the NMO correction is most severe. The waveform of an event in this area is stretched to a longer period as the NMO correction is applied, (Yilmaz, 2001). The amplitude of that event is not affected, but its time distortion is caused by an alteration in its frequency content. Specifically, the lower frequency content is boosted, and since the amplitude of the waveform is maintained, a nonphysical addition of energy to the input signal has occurred. Yilmaz (2001) quantifies the frequency distortion caused by NMO stretch in terms of Δ_{NMO} and t_0 :

$$\frac{\Delta f}{f} = \frac{\Delta_{NMO}}{t_0}, \quad (11)$$

where, f is the dominant frequency of the input waveform. This expression is derived from geometric arguments and assumes $t_0 \gg f^{-1}$, (Yilmaz, 2001). Another approach to describing NMO stretch comes from analyzing the effects of the NMO correction in terms of instantaneous frequency, (Barnes, 1992). This approach provides excellent insight into the frequency distortion, and yields an exact expression for NMO stretch:

$$\beta_B = \frac{t_x}{t_0 - \frac{x^2 v'(t_0)}{v^3(t_0)}}, \quad (12)$$

(Barnes, 1992) where v' is the derivative of v with respect to time. This expression quantifies NMO stretch without approximations, and is not dependent only on the dominant frequency as in equation 11. It is valid for variable velocity models, and for a constant velocity model, the derivative of velocity goes to zero, and $\beta_B - 1$ agrees with the approximation in equation 11, (Barnes, 1992).

In removing the NMO correction, the exact approach must also remove the effects of NMO stretch. As equation 12 suggests, NMO stretch is itself nonstationary, and therefore cannot be removed exactly using stationary filtering theory. However, since the data processing transform takes advantage of nonstationary filtering, NMO stretch can be removed exactly.

Substituting the NMO variables, Δ_{NMO} and α_{NMO} , into the general inverse data processing transform, (Burnett, 2008)

$$F(\beta) = \int_{-\infty}^{\infty} f(p)e^{-i\beta\mathcal{P}(p)} dp. \quad (13)$$

gives the inverse NMO transform:

$$F(\omega) = \int_{-\infty}^{\infty} \alpha_{NMO} h(t_0) e^{-i\omega\Delta_{NMO}(t_0)} e^{-i\omega t_0} dt_0, \quad (14)$$

where the shifting and Fourier exponentials are still separated. Here, insight into the role of α can finally be gained. α_{NMO} is given as,

$$\alpha_{NMO} \equiv \frac{\partial t_x}{\partial t_0} = \frac{t_0 - \frac{x^2 v'(t_0)}{v^3(t_0)}}{t_x}. \quad (15)$$

The inverse NMO transform does account for NMO stretch, and in fact, $\alpha_{NMO} = \beta_B^{-1}$ exactly! Realizing that the two are equivalent leads to a straightforward (once nonstationary filtering is allowed) perspective on predicting and quantifying NMO stretch. Further, Barnes (1992) proves, in terms of instantaneous power and energy spectra, that β_B , and therefore α indeed describes the nonphysical energy change caused by the forward transform. Figure 2 demonstrates how α_{NMO} removes NMO stretch during the inverse NMO transform by appropriately applying nonstationary scaling to the amplitudes.

IMPLEMENTATION

The NMO transform acts as a map between the uncorrected spectrum and the NMO-corrected trace. As such, the first step in implementing the forward NMO transform on a trace is to apply a standard forward Fourier transform to that trace. This gives the uncorrected spectrum, which becomes the input column vector for a matrix vector multiplication. Following the general procedure for matrix operator construction outlined in Burnett (2008), identify the output vector as the time-domain NMO-corrected trace and the transform kernel as $e^{i\omega t_x}$. The input, or horizontal, axis then must be frequency (ω), and the output axis must correspond to NMO-predicted time, t_x . The time sampling interval (δt) must be specified to construct the time axis. The length of the input trace must also be specified to find the frequency sampling interval ($\delta \omega$) and to then construct the frequency axis.

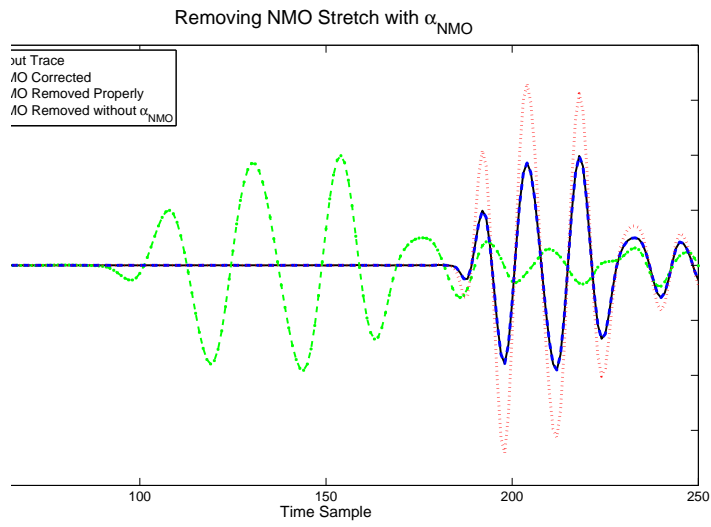


FIG. 2. The effect of α_{NMO} . A single trace ($x=1350\text{m}$, $v(q)$ is linear, 2000-3000m/s) has the NMO transform applied, and then removed two different ways. One way includes the amplitude correction factor, α_{NMO} , and the other does not. Both kinematically remove NMO, but α_{NMO} is needed to account for NMO stretch.

The frequency axis must match the frequency axis used for the Fourier transform, since the matrix operator here will simultaneously remove that Fourier transform as it NMO-corrects the data. The time axis for the forward NMO transform of an N-sample trace is defined as:

$$(t_0)_j = (j - 1)\delta t, \quad (16)$$

for $j=1:N$. To match the MATLAB FFT frequency axis, we define the frequency sampling interval and then the frequency axis respectively as:

$$\Delta\omega = \frac{2\pi}{N\delta t}, \quad (17)$$

and

$$\omega_l = (l - 1)\delta\omega, \quad (18)$$

for $l=1:(1+N/2)$, and

$$\omega_l = (l - N - 1)\delta\omega, \quad (19)$$

for $l=(N/2+2):N$.

Once the discrete axes are constructed, each element of the forward NMO transform operator matrix, \mathbf{A} , can be computed as:

$$a_{jl} \equiv \frac{e^{i\omega_l(t_0)_j}}{2\pi} \circ e^{i\omega_l(\Delta_{NMO})_j} = \frac{e^{i\omega_l(t_x)_j}}{2\pi}, \quad (20)$$

where,

$$(t_x)_j = \sqrt{(t_0)_j^2 + \frac{x^2}{v_j^2}}. \quad (21)$$

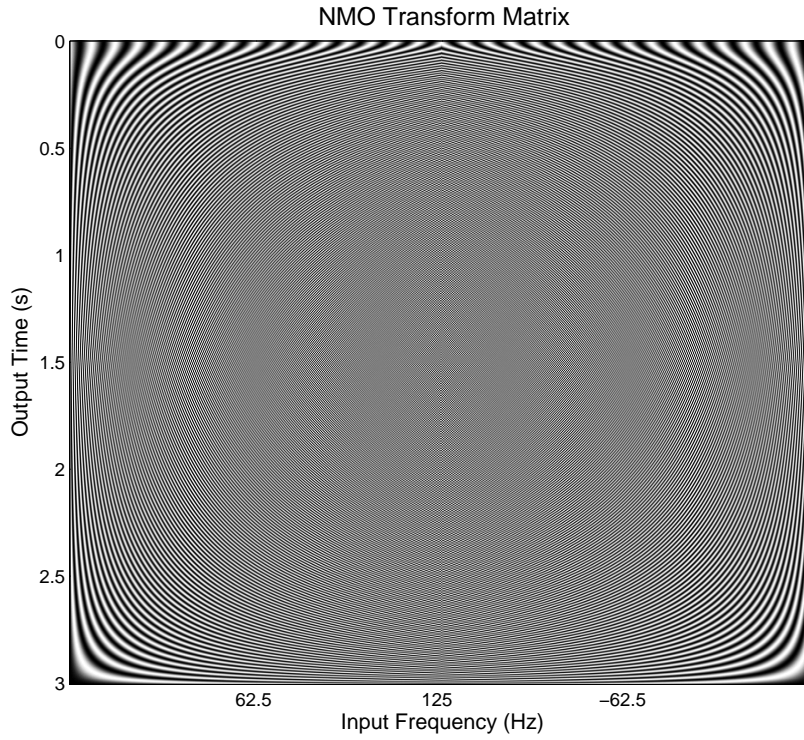


FIG. 3. The real part of a single NMO transform operator matrix. Multiplication of this matrix with a frequency spectrum gives the NMO-corrected time series associated with that spectrum. This matrix changes for each trace unless the offset and the velocity model are held constant.

The NMO transform is then expressed as a matrix vector multiplication:

$$h\left((t_0)_j\right) = \sum_{l=1}^N a_{jl} F(\omega_l). \quad (22)$$

An example of a full matrix operator for the forward NMO transform is shown in Figure 3. The matrix in Figure 3 is the Hadamard (entry-wise) product of an ordinary inverse Fourier transform matrix and the forward shifting matrix. Figure 5 shows the two matrices side by side. Although not immediately clear in figure 3, figure 5 shows that both parts of the operator have symmetry over the frequency axis, and expense can immediately be saved by only computing the positive-frequency half of the matrix and copying values to the negative half. Any increase in computational efficiency is valuable, as for a trace of length N , N^2 operations are required to perform the full matrix vector multiplication.

The inverse NMO transform uses the NMO-corrected time series as its input vector, and the uncorrected spectrum as its output vector. The same axes will be used as in the forward transform, except they will switch input and output roles, making time defined over the l -index, and frequency over the j -index. Each element of the inverse NMO transform kernel, \mathbf{B} , is then computed as

$$b_{jl} \equiv (\alpha_{NMO})_l e^{-i\omega_j(t_0)_l} \circ e^{-i\omega_j(\Delta_{NMO})_l} = \alpha_l e^{-i\omega_j(t_x)_l}, \quad (23)$$

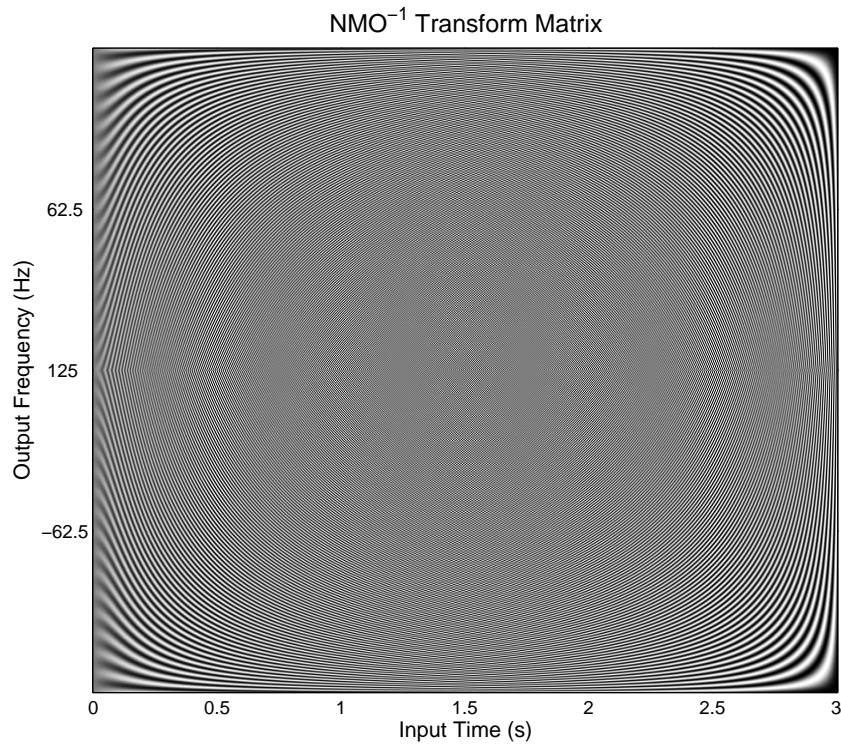


FIG. 4. The real part of a single NMO^{-1} transform operator matrix. This is the inverse of the matrix shown in figure 3. Multiplication of this matrix with a trace recovers the uncorrected spectrum of that trace.

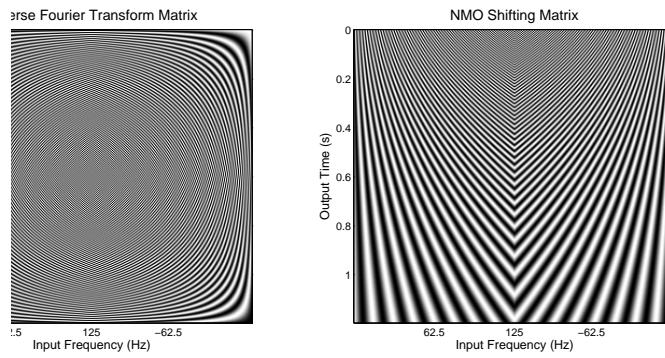


FIG. 5. An example NMO transform matrix separated into its inverse Fourier transform and forward shifting matrices. Only the real part is shown. The symmetry about the frequency axis is clear. The Hadamard (entry-wise) product of these two matrices gives the mixed-domain NMO operator matrix. An example of the full operator matrix is shown in figure 3.

no summation over l . Implementing α_{NMO} requires a derivative of velocity to be computed. This is one area that can introduce error into the discrete inverse transform. Since the matrix vector multiplication is already quite expensive, it is probably worthwhile in most cases to employ an accurate derivative algorithm. However, in many real situations, the velocity function can be a stepping function, where the derivative is undefined at the jumps in the function. In these cases, it is often better to assume an interval-wise constant velocity (for α_{NMO} only) and be aware that error may be introduced here for inverse NMO. Assuming a velocity function with a defined derivative, α_{NMO} is discretely expressed as:

$$(\alpha_{NMO})_l = \frac{(t_0)_l - \frac{x^2 v'((t_0)_l)}{v^3((t_0)_l)}}{(t_x)_l}. \quad (24)$$

The inverse NMO transform can now be expressed as a matrix vector multiplication:

$$F(\omega_j) = \sum_{l=1}^N b_{jl} h((t_0)_l). \quad (25)$$

The matrix operator can be displayed and examined for symmetry. Figure 4 shows the full inverse NMO operator for the same trace as Figure 3. This can again be expressed as the Hadamard product of a regular Fourier transform matrix and the reverse shifting matrix, scaled along the time axis by α_{NMO} . The separated version is shown in Figure 6, where symmetry is again clear over the frequency axis.

DISCUSSION

NMO can be applied by matrix vector multiplication in the time-domain as well, (Claerbout, 1992). Just as the NMO transform accomplishes in the mixed-domain, the time domain NMO matrix is a variably shifted Dirac delta function. However, in the time-domain alone, reversing the NMO correction is difficult for variable velocity models. The input axis of the forward transform in the time domain corresponds to t_x and the output axis is t_0 , while the roles are reversed for the inverse transform. The problem with this approach in the time domain is that the delta function must be discretely approximated. Instead of

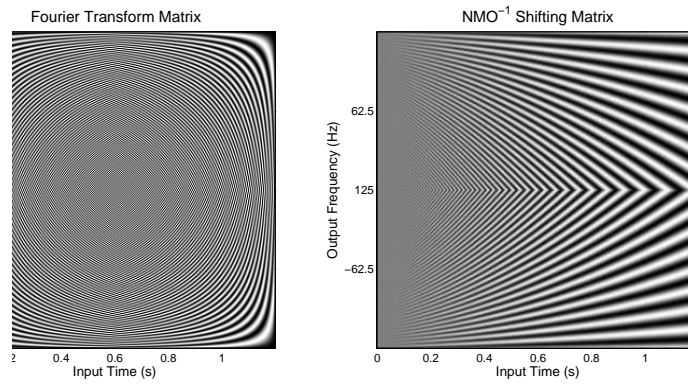


FIG. 6. An example NMO^{-1} transform matrix separated into its Fourier transform and reverse shifting matrices. Only the real part is shown. The Hadamard product of these two matrices gives the mixed-domain NMO^{-1} operator. Again, the symmetry is clear over the frequency axis.

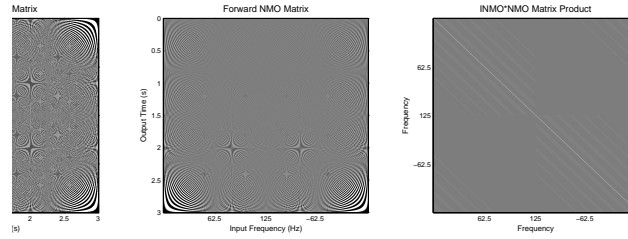


FIG. 7. The matrix product of the NMO^{-1} and NMO matrices for a single trace. Their product should give the identity matrix (zero, except for ones along the diagonal) if the inverse is perfect. Only a small amount of energy is off of the diagonal.

an impulse, an interpolator function is substituted, (Claerbout, 1992). Even a bandwidth-friendly interpolator choice such as the sinc function is difficult to accurately implement on the grid of the time domain.

By applying NMO through the mixed-domain, the matrix vector implementation of the transform gives a band-limited approximation to convolution with a continuous Delta function that is not confined to only the rigid time sampling grid. Instead of extracting an interpolated value based on some assumed behaviour between samples, the exact value of the continuous band-limited version of the recorded function is extracted. Since this entire continuous function is defined exactly by the frequency spectrum of the actual recorded data, both the original sample values and the target values are preserved throughout the transform process. For these reasons, the mixed domain NMO transform is almost exactly reversible, even in practise. An estimate of how well the inverse NMO transform is approximated is shown in figure 7. The inverse NMO transform matrix times the forward NMO transform matrix approximates the identity matrix, \mathbf{I} , quite well.

Another practical test for evaluating how well the NMO transform and its inverse perform is shown in figures 8, 9, and 10. In all three, the input data is shown in the left panel. The central panel shows the NMO correction applied in figure 8 and removed in figure 9 using a conventional 5-point sinc-interpolation algorithm. The velocity model for the NMO correction linearly increases from 2000 and 3000 m/s from the top to the bottom of the section. The right panels in figures 8 and 9 show the same process repeated using the

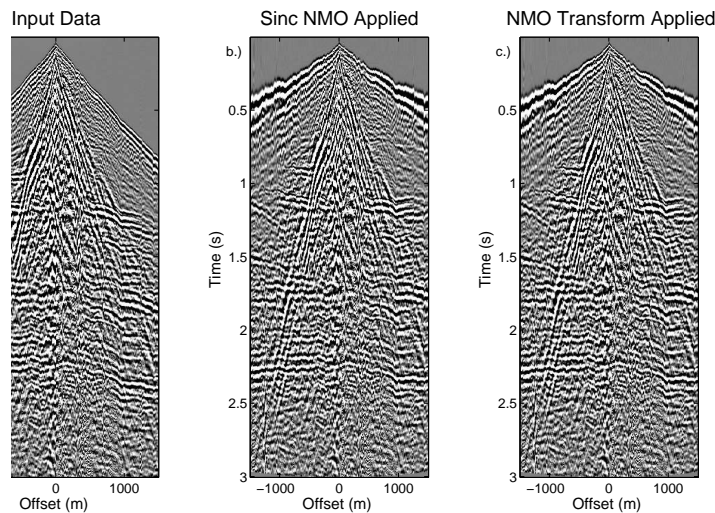


FIG. 8. NMO method comparison. The NMO correction for a linearly increasing velocity model is applied to the input data (a.) using a conventional 5-point sinc-interpolation algorithm (b.) and the NMO transform (c.).

NMO and NMO^{-1} transform. The results for the forward and inverse NMO are visually indistinguishable between methods, suggesting that the transform method would not influence interpretation of the final image. However, figure 10 shows the difference section for both NMO , NMO^{-1} processing sequences, and there is a noticeable difference. The difference panels are scaled by 100 times the input data to show that a percentage of the data is lost under the sinc-interpolation sequence. The transform sequence is much cleaner, with some ringing in the difference section caused by the variable velocity model. Near the top of the section, where NMO stretch is severe, neither algorithm recovers the data well. In most real cases, this shallow data is not of interest to reflection processing as it contains mostly direct arrivals, very shallow reflections, and refractions.

ACKNOWLEDGEMENTS

The Jackson School of Geosciences, University of Texas at Austin, the EDGER Forum, and the sponsors of CREWES for supporting this research.

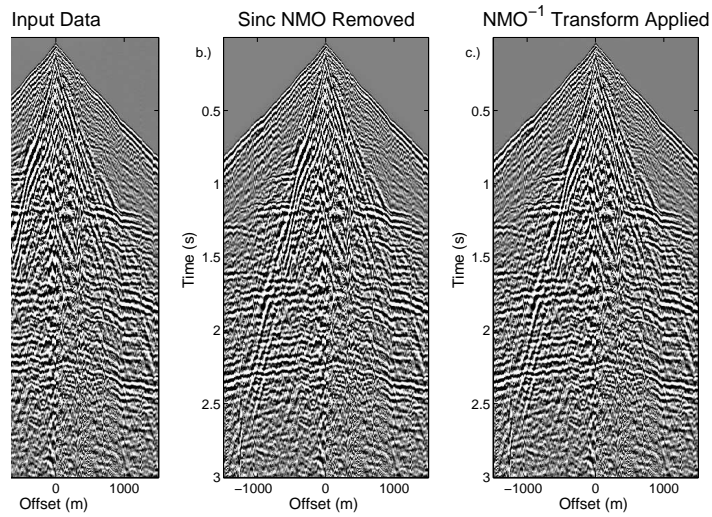


FIG. 9. NMO^{-1} method comparison. The NMO correction is removed from the results shown in figure 8 using a 5-point sinc-interpolation algorithm (b.) and the NMO^{-1} transform (c.). The results should ideally recover the input data (a.) exactly. Both methods visually appear to give the same result, although this is not really the case (see figure 10).

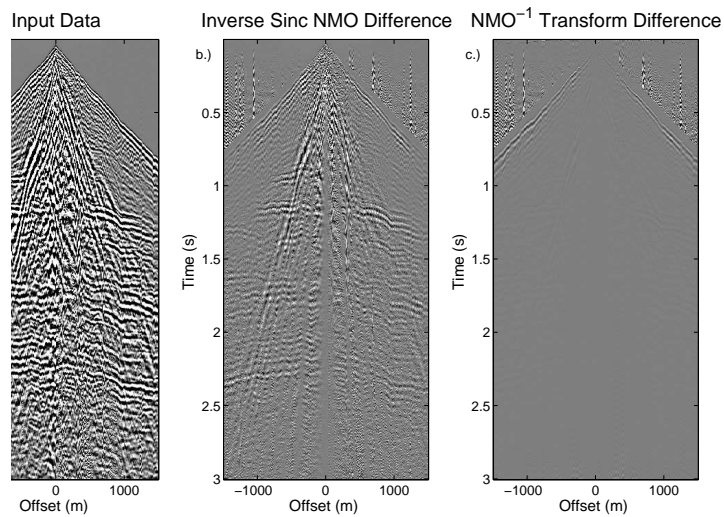


FIG. 10. NMO methods difference comparison. Difference sections after the NMO correction is applied and removed from the input data (a.), using (b.) a 5-point sinc-interpolation algorithm and (c.) the NMO/NMO^{-1} transform. Panels (b.) and (c.) are normalized to the maximum of the input data and scaled by 100, showing that the conventional sinc-interpolation sequence destroys a percentage of the useful data.

REFERENCES

- Alkhalifah, T., 1997, Velocity analysis using nonhyperbolic moveout in transversely isotropic media: *Geophysics*, **62**, 1839–1854.
- Barnes, A. E., 1992, Another look at nmo stretch: *Geophysics*, **57**, 749–751.
- Buchholtz, H., 1972, A note on signal distortion due to dynamic (nmo) corrections: *Geophysical Prospecting*, **20**, 395–402.
- Burnett, W. A., 2007, A general transform for reversible seismic data processing by nonstationary filtering: Ph.D. thesis, University of Texas, Austin.
- Burnett, W. A., 2008, A reversible transform for seismic data processing: *CREWES Research Report*, **20**, 1–17.
- Claerbout, J. F., 1992, *Earth Soundings Analysis: Processing versus Inversion*: Blackwell Science.
- Dobrin, M., and Savit, C., 1988, *Introduction to Geophysical Prospecting*: McGraw-Hill Inc.
- Dunkin, J. W., and Levin, F. K., 1973, Effect of normal moveout on a seismic pulse: *Geophysics*, **38**, 635–642.
- Tsvankin, I., and Thomsen, L., 1994, Non-hyperbolic reflection moveout in anisotropic media: *Geophysics*, **59**, 1290–1304.
- Yilmaz, O., 2001, *Seismic Data Analysis*: Society of Exploration Geophysics.